Top Catal (2008) 50:124–132
DOI 10.1007/s11244-008-9099-7

ORIGINAL PAPER

Autoxidation of Hydrocarbons: From Chemistry to Catalysis

Ive Hermans · Jozef Peeters · Pierre A. Jacobs

Published online: 13 June 2008

Abstract This contribution summarizes our recent efforts to unravel the radical chemistry of autoxidations. Abstraction of the weakly bonded αH-atom of the primary hydroperoxide product by chain carrying peroxyl radicals is identified as the source of major end products such as alcohol and ketone/aldehyde. In the case of cyclohexane autoxidation, this reaction is even responsible for the majority of ring-opened by-products. In a second part, different approaches to autoxidation catalysis are discussed, ranging from transition metal ion catalysis to organocatalysis with immobilized *N*-hydroxyphthalimide.

Keywords Catalyst immobilization · Kinetics · Mechanism · Radicals

1 Introduction

Autoxidation chemistry plays a pivotal role in the chemical industry as it upgrades relatively cheap hydrocarbons to value-added oxygenated products [1–4]. Important examples are for instance the oxidation of cyclohexane to cyclohexanone and cyclohexanol (6×10^6 annual tons), the synthesis of terephthalic acid from *p*-xylene (30×10^6 annual tons) and the oxidation of cumene to cumene hydroperoxide (5×10^6 annual tons), the first step in the production of phenol. Advantageously, these processes use molecular oxygen as the terminal oxidant, rather than expensive and/or noxious alternatives. Unfortunately, the underlying radical mechanism is not always as selective as desired, often leading to by-products, even at low conversions. This is especially the case for cyclohexane autoxidation where the conversion is industrially limited to less than 5% in order to avoid the formation of large quantities of ring-opened by-products. Therefore cyclohexane is an interesting model substrate to study the autoxidation mechanism. Indeed, despite the industrial relevance, the radical chemistry of these processes remained poorly understood for several decades. Generally, autoxidation chemistry has long been explained by reactions (1–6) [1–4].

$$\mathrm{ROOH} \rightarrow \mathrm{RO}^{\bullet} + {}^{\bullet}\mathrm{OH} \quad (1)$$

$$\mathrm{RO}^{\bullet} + \mathrm{RH} \rightarrow \mathrm{ROH} + \mathrm{R}^{\bullet} \quad (2)$$

$${}^{\bullet}\mathrm{OH} + \mathrm{RH} \rightarrow \mathrm{H_2O} + \mathrm{R}^{\bullet} \quad (3)$$

$$\mathrm{R}^{\bullet} + \mathrm{O_2} \rightarrow \mathrm{ROO}^{\bullet} \quad (4)$$

$$\mathrm{ROO}^{\bullet} + \mathrm{RH} \rightarrow \mathrm{ROOH} + \mathrm{R}^{\bullet} \quad (5)$$

$$\mathrm{ROO}^{\bullet} + \mathrm{ROO}^{\bullet} \rightarrow \mathrm{ROH} + \mathrm{Q{=}O} + \mathrm{O_2} \quad (6)$$

Reaction (1) is the homolytic dissociation of a hydroperoxide molecule (ROOH) into oxygen-centered alkoxy ($\mathrm{RO}^{\bullet}$) and hydroxyl (${}^{\bullet}\mathrm{OH}$) radicals. In absence of a catalyst, this reaction was assumed to be the dominant chain-initiation reaction, rationalizing why traces of ROOH are often

I. Hermans · P. A. Jacobs
Centre for Surface Chemistry and Catalysis, Department of Microbial and Molecular Systems (M2S), K.U.Leuven, Kasteelpark Arenberg 23, 3001 Leuven, Belgium
URL: www.humans.ethz.ch

I. Hermans (✉)
Department of Chemistry and Applied Biosciences, Institute for Chemical and Bioengineering, Swiss Federal Institute of Technology (ETH Zürich), Hönggerberg, HCI, Wolfgang-Pauli-Str. 10, 8093 Zurich, Switzerland
e-mail: ive.hermans@chem.ethz.ch
URL: www.humans.ethz.ch

J. Peeters
Department of Chemistry, K.U.Leuven, Celestijnenlaan 200F, 3001 Leuven, Belgium

initially added to the alkane substrate to light-off the reaction. Both the RO$^{\bullet}$ and $^{\bullet}$OH radicals react very fast with the substrate (reactions 2 and 3) to produce alkyl radicals (R$^{\bullet}$). These species add oxygen in a diffusion controlled reaction (4), producing peroxyl radicals (ROO$^{\bullet}$), able to abstract H-atoms from the substrate, thereby producing hydroperoxide and regenerating the alkyl radical (reaction 5). Reactions (4) and (5) form a propagation cycle which is repeated many times before peroxyl radicals are destroyed in a mutual termination reaction (6), yielding an equimolar amount of alcohol (ROH) and ketone (Q=O). This termination reaction is compensating the initiation reaction, leading to a quasi steady-state in peroxyl radicals. The ratio between the rate of propagation and termination is the so-called chain length and is generally accepted to be a large number (i.e., >10) [1]. This simple reaction scheme thus attributes ROOH to a fast propagation reaction whereas Q=O would only originate in a much slower termination step; alcohol is additionally produced in a fast alkoxy abstraction reaction (2), subsequent to the slow initiation reaction. This view is however contradicted by the experimental alcohol and ketone yields being of the same order of magnitude as the ROOH yield. Moreover, the negative second derivative of the ROOH evolution and the positive second derivative of the ROH and Q=O evolutions as a function of the sum of products (Fig. 1) unambiguously identify ROOH as primary, and ROH and Q=O as secondary products, respectively [5, 6]. During cyclohexane autoxidation, the ROOH yield even goes through a maximum, pointing to a destruction mechanism which becomes faster than the formation reaction (5) (see Fig. 1). Nevertheless, such a reaction is missing in the textbook mechanism outlined above.

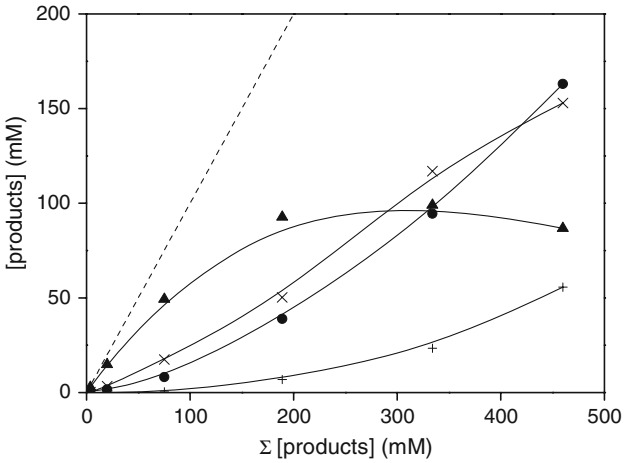

Fig. 1 Evolution of the cyclohexane autoxidation products at 130 °C as a function of the sum of products: CyOOH (▲), CyOH (×), Q=O (●), by-products (+). The dashed line represents the sum of products

2 The Formation of Radicals

Chain initiation reaction (1) is another weak point in the established reaction scheme. This reaction is indeed not only very slow, due to its 40 kcal mol^{-1} energy barrier, it is also highly inefficient in generating radicals in the liquid phase. Indeed, the nascent RO$^{\bullet}$ and $^{\bullet}$OH radicals will rather recombine within their Franck–Rabinowitch solvent-cage (Fig. 2) than to diffuse away from each other, a process which faces a diffusion barrier due to their mutual attraction [7].

Nevertheless, radicals are formed, and especially during the autoxidation of cyclohexane the rate of the initiation is known to even increase significantly during the reaction [7]. We were able to experimentally measure the pseudo-first-order rate constant of the initiation process during cyclohexane autoxidation and found it proportional to the initially added Q=O concentration. This correlation characterizes and kinetically quantifies a bi-molecular reaction between CyOOH and cyclohexanone as initiation mechanism. Different reactions were proposed and the rate of them predicted from first principles, based on detailed transition state theory calculations. The most likely mechanism, sustaining all experimental observations, is a reaction in which the $^{\bullet}$OH-radical breaking away from the CyO–OH molecule abstracts a weakly bonded αH-atom from cyclohexanone (reaction 7, Fig. 2) [7].

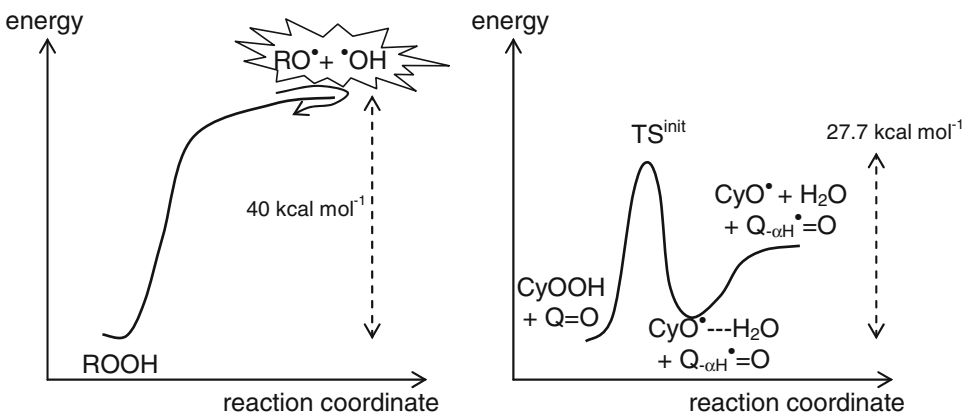

Fig. 2 Evolution of the potential energy as a function of the reaction coordinate for reactions (1) and (7) [7]

$$CyOOH + Q{=}O \rightarrow CyO^{\bullet} + H_2O + Q^{\bullet}_{-\alpha H}{=}O \quad (7)$$

Reaction (7) is not only faster than reaction (1) due to its loose and energetically low transition state, the reaction is also more efficient in generating free radicals because in-cage recombination is hampered among others by resonance stabilization in the ketonyl product radical ($Q^{\bullet}_{-\alpha H}{=}O$). Therefore, during the main part of the cyclohexane autoxidation, initiation takes place via reaction (7). Because of the sharp Q=O concentration increase during cyclohexane autoxidation, the initiation rate also increases rapidly, leading to the observed autocatalytic up-swing. At low CyH conversion, where [Q=O] is still low, a similar but significantly slower initiation mechanism takes place with the alkane substrate (reaction 8) featuring a barrier of 28.8 kcal mol^{-1}, i.e., 1.1 kcal mol^{-1} higher than for reaction (7) [7]. An analogous mechanism is also the dominant radical source throughout ethylbenzene oxidation as no products are formed which exhibit a major lighting-off potential as cyclohexanone [8]. The latter also explains why the ethylbenzene conversion does not increase exponentially as a function of time as the cyclohexane conversion does.

$$ROOH + RH \rightarrow RO^{\bullet} + H_2O + R^{\bullet} \quad (8)$$

3 The Formation of the Alcohol and Ketone Products

Besides elucidating the initiation mechanisms of autoxidations, we were also interested to unravel the reaction paths leading to products. A combined experimental and theoretical investigation pointed out that the ROOH product reacts significantly faster with the chain-carrying peroxyl radicals than the RH substrate itself. E.g., k^{ROOH}/k^{RH} was found to be 55 for cyclohexane [5, 6], 20 for toluene [9] and 10 for ethylbenzene [8]. Therefore we were keen to find out which products are produced after this fast αH-abstraction from ROOH. A theoretical investigation demonstrated that the initially formed $R_{-\alpha H}{}^{\bullet}OOH$ radical (reaction 9) is unstable and promptly dissociates to the corresponding carbonyl compound plus $^{\bullet}OH$ (reaction 10), without any barrier [10]. The hitherto overlooked ROOH co-propagation could therefore be identified as a fast and straightforward source of ketone or aldehyde, depending on the substrate.

$$ROO^{\bullet} + ROOH \rightarrow ROOH + R^{\bullet}_{-\alpha H}OOH \quad (9)$$

$$R^{\bullet}_{-\alpha H}OOH \rightarrow Q{=}O + {}^{\bullet}OH \quad (10)$$

Subsequent to the exothermic dissociation (10), the co-produced $^{\bullet}OH$ radical will abstract an H-atom from the RH substrate forming the wall of the solvent-cage around the {ROOH + Q=O + $^{\bullet}OH$} products (reaction 11). This abstraction reaction produces additional heat, putting the overall exothermicity of the ROOH propagation at about 50 kcal mol^{-1} [5]. This heat will cause the formation of a nano-sized hot-spot which lasts for a few picoseconds before heat diffusion thermalizes the system. During this short period, the {ROOH + $R^{\bullet}$ + Q=O + H_2O} products can either diffuse away from each other (reaction 12), or the alkyl radical can abstract the OH group of the nascent ROOH molecule (reaction 13). The diffusive separation (12) features a lower energy barrier than cage reaction (13), but by its "Brownian" nature the former also exhibits a much lower frequency factor [5, 6]. Hence, due to the temperature activation, competition can take place.

$$\{ROOH + Q{=}O + {}^{\bullet}OH\}^{cage} + RH^{cage-wall} \rightarrow \{ROOH + R^{\bullet} + Q{=}O + H_2O\}^{cage} \quad (11)$$

$$\{ROOH + R^{\bullet} + Q{=}O + H_2O\}^{cage} \rightarrow ROOH + R^{\bullet} + Q{=}O + H_2O \quad (12)$$

$$\{ROOH + R^{\bullet} + Q{=}O + H_2O\}^{cage} \rightarrow \{RO^{\bullet} + ROH + Q{=}O + H_2O\}^{cage} \quad (13)$$

Based on a detailed stoichiometric and kinetic analysis of the product distributions obtained with various substrates, the reaction flux going through cage-channel (13) could be evaluated experimentally. The cage efficiency follows the stability of the corresponding alkyl radical, as expected: 70% for cyclohexane [5, 6], 56% for toluene [9] and 22% for ethylbenzene [8], respectively. Cage channel (13) could therefore not only be identified as the dominant source of ROH in all investigated autoxidation systems, it also causes a net removal of ROOH, explaining why the CyOOH yield is decreasing at high CyH conversion (Fig. 1). Note that the lower efficiency of reaction (13) for ethylbenzene, compared to cyclohexane, also explains the significantly higher Q=O/ROH ratio observed with this substrate [8].

Co-propagation of the alcohol product proceeds preferentially by the abstraction of the αH-atom (reaction 14) [5, 6]. Although slower than the αH-abstraction from the hydroperoxide (e.g., $k^{CyOOH}/k^{CyOH} \approx 5.5$), this reaction is still important and puts its mark on the overall chemistry. Indeed, addition of O_2 to the α-hydroxy-alkyl radical yields an α-hydroxy-alkylperoxyl radical (reaction 15). Hitherto this radical was assumed to react as other peroxyl radicals, abstracting H-atoms from the substrate and terminating with peroxyl radicals. However, we discovered a much faster unimolecular decomposition path for this $Q(OH)OO^{\bullet}$ radical (reaction 16) [11], producing $HO_2^{\bullet}$ radicals.

$$ROO^{\bullet} + ROH \rightarrow ROOH + R^{\bullet}_{-\alpha H}OH \quad (14)$$

$$R^{\bullet}_{-\alpha H}OH + O_2 \rightarrow Q(OH)OO^{\bullet} \quad (15)$$

$$Q(OH)OO^{\bullet} \rightarrow Q{=}O + HO_2^{\bullet} \quad (16)$$

At low conversion (where the $ROO^{\bullet}$/RH ratio is still low) the $HO_2^{\bullet}$ radicals will mainly react with the substrate (reaction 17), whereas at higher conversions (viz. higher $ROO^{\bullet}$ concentrations), $HO_2^{\bullet}$ will predominantly react diffusion

controlled with peroxyl radicals in a head-to-tail termination reaction (reaction 18) [12].

$$HO_2^{\bullet} + RH \rightarrow H_2O_2 + R^{\bullet} \quad (17)$$

$$HO_2^{\bullet} + ROO^{\bullet} \rightarrow O_2 + ROOH \quad (18)$$

This is important for the autoxidation mechanism as reaction (18) will slow down the overall rate. So whereas during cyclohexane autoxidation cyclohexanone enhances the oxidation rate [7], co-oxidation of cyclohexanol inhibits the process.

Theoretical calculations suggest that reaction (23) would be slightly favored over reaction (22) [14]. The alkoxy radical thus produced will mainly react with the cyclohexane substrate and yields 6-hydroxyhexanoic acid (reaction 24) as β-C–C cleavage is unimportant for this oxy radical [15].

(24)

4 Formation of Ring-opened By-products During Cyclohexane Autoxidation

The $RO^{\bullet}$ radicals co-produced in cage-reaction (13) can in the case of cyclohexane not only react with the alkane substrate (reaction 2), but also decompose via β-C–C scission (19), producing ω-formyl radicals [13].

$$CyO^{\bullet} \rightarrow {}^{\bullet}CH_2-(CH_2)_4-CHO \quad (19)$$

These $^{\bullet}CH_2$–$(CH_2)_4$–CHO radicals will rapidly add O_2 and yield $^{\bullet}OOCH_2$–$(CH_2)_4$–CHO radicals (reaction 20), able to isomerize according to reaction (21) [14].

The $HOOCH_2$–$(CH_2)_4$–$C(=O)OO^{\bullet}$ radical, although formed in a lower quantity, will react with the substrate, producing a nascent peracid (reaction 25). A fast, highly exothermic, subsequent cage-reaction (26) transforms this peracid into an acyloxy radical which can either diffuse away from its CyOH cage-partner (reaction 27), or undergo a second, activated, cage-reaction (reaction 28) [16].

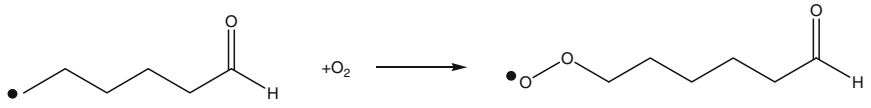

(20)

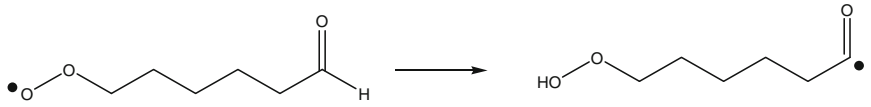

(21)

Next there is competition between addition of O_2 to this acyl radical (reaction 22) and a unimolecular 1,7-OH-shift (reaction 23).

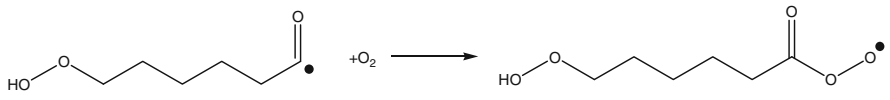

(22)

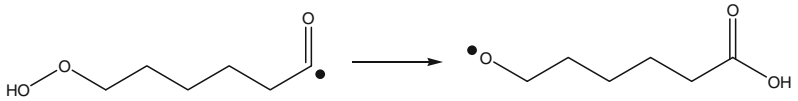

(23)

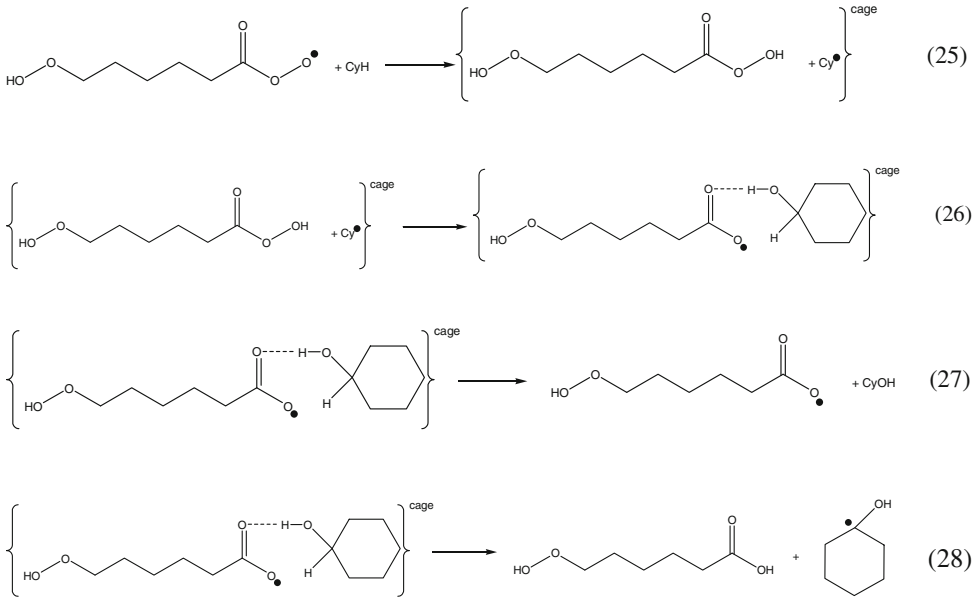

whereas the diffusive separation (27) will ultimately result in decarboxylation (reaction 29), cage-reaction (28) yields 6-hydroperoxy-hexanoic acid, another minor by-product, observed experimentally.

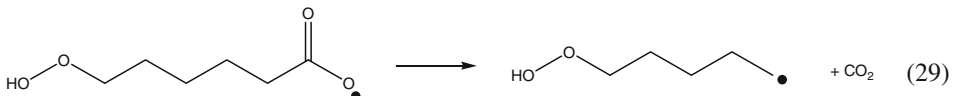

Important to emphasize is the fact that 6-hydroxyhexanoic acid (and to a minor extend also 6-hydroperoxy-hexanoic acid) could be identified experimentally as the most important primary by-product [14]. Indeed subsequent oxidation of this 6-hydroxyhexanoic acid (and 6-hydroperoxide-hexanoic acid) results in the formation of other (decarboxylated) side-products. $CyO^{\bullet}$ radicals, produced in the CyOOH propagation, are thus straightforwardly transformed to (decarboxylated) by-products via the intermediate stage of 6-hydroxy- and 6-hydroperoxy-hexanoic acids (Fig. 3). CyOOH could thus be identified as the most important precursor of by-products, rather than cyclohexanone as assumed in the literature [14]. Indeed, due to the 10 times higher reactivity of CyOOH compared to Q=O, and the CyOOH/Q=O ratio being larger than unity, 80% of by-products stem from CyOOH and only 20% from Q=O during the thermal autoxidation process.

5 Catalysis by Transition Metal Ions

It is known that transition metal ions which are able to undergo a one-electron switch (e.g., $Co^{2+/3+}$) significantly enhance the rate of autoxidations, even at low concentrations [1–4]. Such metals indeed catalyze the initiation reaction via a so-called Haber–Weiss cycle (presumably reactions 30 and 31).

$$Co(II) + CyOOH \rightarrow Co(III)OH + CyO^{\bullet} \quad (30)$$

$$Co(III)OH + CyOOH \rightarrow Co(II) + CyOO^{\bullet} + H_2O \quad (31)$$

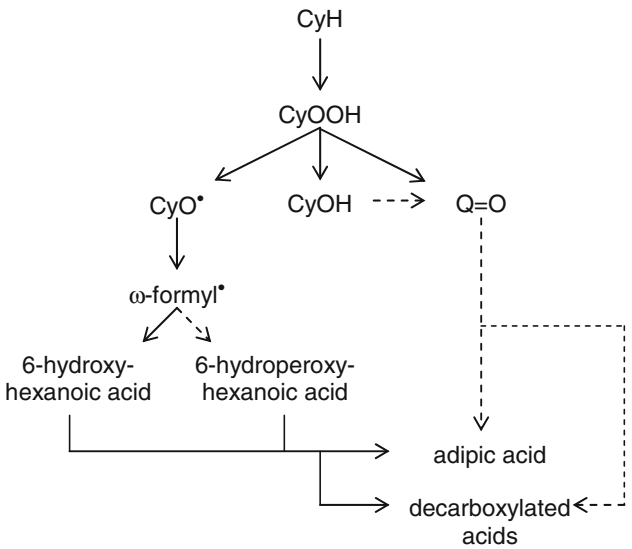

Fig. 3 Formation of (by-)products during the autoxidation of cyclohexane. Minor routes are indicated with dashed lines

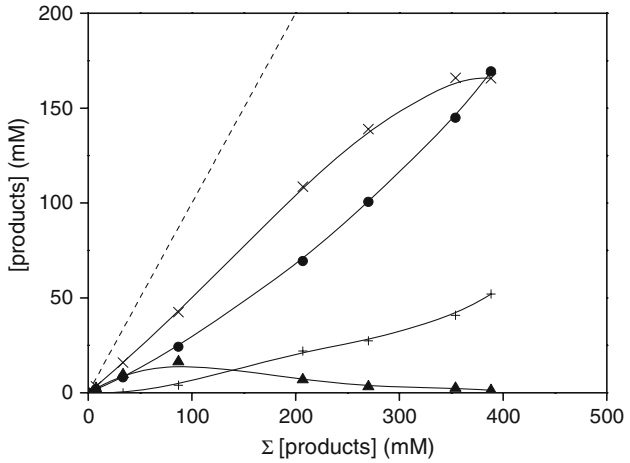

Fig. 4 Evolution of the cyclohexane autoxidation products at 130 °C in the presence of 5 ppm $Co(acac)_2$ as a function of the sum of products: CyOOH (▲), CyOH (×), Q=O (●), by-products (+). The dashed line represents the sum of products

Reactions (30) and (31) do not only take over the role of chain initiations (7) and (8) but are also responsible for the conversion of CyOOH, rather than reactions (9–13). Important to emphasize is that this catalyzed CyOOH destruction also produces $CyO^{\bullet}$ radicals, analogous to the $CyOO^{\bullet}$ induced removal discussed above. A significant part of these $CyO^{\bullet}$ radicals is converted to by-products, analogous to the thermal system. It thus seems that Co(II) ions only cause a slight perturbation of the autoxidation chemistry (see Fig. 4) [16]. Indeed, also for the $Co(acac)_2$ catalyzed cyclohexane autoxidation, 6-hydroxyhexanoic acid could also be identified as the most important primary by-product from which the majority of other (decaroxylated) by-products originate.

Chromium ions offer even more opportunities as they can additionally catalyze the dehydration of hydroperoxides to ketones [1, 17]. This way, one would be able to achieve an in situ deperoxidation to cyclohexanone, the most desired product which is moreover acting as an autocatalyst in cyclohexane autoxidation (vide supra). Unfortunately, chromium and especially Cr(VI) is too noxious to be used in a homogeneous process and immobilization is an important prerequisite for its industrial use. Whereas Co ions can for instance be readily substituted for Al ions in $AlPO_4$-n materials [18, 19], immobilization of Cr appears more difficult. Indeed, many of the reported Cr materials turned out to be unstable under the harsh autoxidation conditions and were just slowly releasing Cr as a homogeneous catalyst [20]. Based on state-of-the-art colloid chemistry, and inspired by the low solubility of Cr_2O_3, we suceeded in the design of a heterogeneous Cr catalyst for cyclohexane autoxidation [21]. In this approach, in situ generated nano-sized Cr(III) colloids are immediately immobilized onto an inert support material, freezing the dispersion and avoiding aggregation. By modifying physico-chemical immobilization parameters, the size of the Cr(III) particles can be tuned between about 2 and 1,000 nm [22]. Whereas the smallest particle range corresponds to elementary building block colloids, the larger, secondary particles can arise by aggregation of the small primary particles prior to their immobilization. These materials were demonstrated to be stable and selective catalysts for cyclohexane autoxidation, causing a nearly complete deperoxidation and a significant boost in Q=O yield, even if only added in 5 ppm [21].

Nevertheless, both with $Cr(acac)_3$ and immobilized Cr(III) colloids, all (by-)products appear to be primary, significantly different from the overall product evolution in the thermal or the cobalt catalyzed systems [16]. This suggests that, besides a Haber–Weiss cycle, Cr(III) ions are also able to catalyze additional steps, some of them directly leading to by-products. Currently these catalytic steps are under investigation.

6 Organocatalysis by *N*-hydroxyphthalimide

In principle one could not only catalyze the chain initiation (vide supra), but also the chain propagation. An approach that received a great deal of attention recently is the use of *N*-hydroxyphtalimide (NHPI) or other appropriate *N*-hydroxyimides (>NOH) [23–43]. Under autoxidation conditions, NHPI is partially converted to phthalimide-*N*-oxyl radicals ($PINO^{\bullet}$) by an equilibrated reaction with peroxyl radicals (reaction 32) [44].

$$ROO^{\bullet} + NHPI \leftrightarrows ROO\text{-}H + PINO^{\bullet} \quad (32)$$

These $PINO^{\bullet}$ radicals are found to abstract H-atoms from the RH substrate (reaction 33) even faster than $ROO^{\bullet}$ radicals, although the O–H bond strength is not significantly higher in NHPI than in ROO-H [43–45].

$$PINO^{\bullet} + RH \rightarrow NHPI + R^{\bullet} \quad (33)$$

Moreover, $PINO^{\bullet}$ radicals terminate much more slowly than peroxyl radicals (cfr. reaction 6), making them more efficient chain carriers. Addition of NHPI thus causes an increase in the radical concentration, and yields more reactive radicals. Both these effects together give NHPI and related compounds its unique catalytic properties.

The Catalytic Efficiency (C.E.) of NHPI catalyzed autoxidations can be approximated by Eq. 1 where k^{33} and k^5 represent the rate constants of reactions (33) and (5), respectively, and $K_{eq,32}$ the equilibrium constant of reaction (32) [44].

$$\text{C.E.} = 1 + k^{33}/k^{5} \times K_{\text{eq},32} \times [\text{NHPI}]/[\text{ROOH}] \qquad \text{(Eq.1)}$$

According to this equation, a suitable *N*-hydroxyimide catalyst should have a strong >NO–H bond to allow fast H-abstraction from the substrate by the corresponding >NO$^{\bullet}$ radical, but not too strong as this would shift equilibrium (32) too far towards the less efficient ROO$^{\bullet}$ radicals. It turns out that more, but, as a consequence, slightly less reactive nitroxyl radicals often result in a better catalytic performance [45]. However, if the >NO–H bond in the *N*-hydroxyimide is too weak, the nitroxyl radicals become radical traps, rather than catalysts.

Unfortunately, NHPI could only be used in homogeneous conditions, dissolved in a polar solvent. Due to its cost, recycling of this organocatalyst remained a difficult hurdle. Until recently, there was only one heterogeneous NHPI system reported in the literature, still operating in acetic acid as a solvent [46]. Therefore we aimed for the design of a solvent-free heterogeneous NHPI system [47].

In our approach, the polar NHPI was impregnated on inert support materials, i.e., silica and silica-alumina gels. In an evaluation of the performance of these materials in the autoxidation of cyclohexane, a strong correlation with the polarity of the support surface was observed. Materials with a high surface density of hydroxyl groups, determined by ^{29}Si MAS NMR, were found to deactivate very fast [47]. Supports with a low fraction of hydroxyl groups were found to act as truly heterogeneous and recyclable catalysts, although during the first recycle some loss in activity could be observed. This decreased activity was associated with the appearance of adsorbed adipic acid, evidenced by FTIR spectroscopy, probably causing screening of the active sites. After the initial activity decrease, the conversion remains steady and no additional adipic acid seems to be adsorbed. When the catalyst was withdrawn from the liquid phase just below the boiling point of the substrate, the autoxidation was observed to first come to a standstill, and to take off again only after a long induction period (Fig. 5). If the catalytic activity would stem from NHPI leached into the liquid phase, it would obviously remain unchanged after removal of the catalyst. All these observations strongly support the heterogeneous nature of the catalysis.

The immobilized-NHPI system was also used to study the influence of PINO$^{\bullet}$ propagators on the product distribution. Indeed, PINO$^{\bullet}$ reacts even faster with CyOOH than ROO$^{\bullet}$ radicals, causing a stoichiometric conversion of CyOOH (reaction 34) [47].

$$\text{PINO}^{\bullet} + \text{CyOOH} \rightarrow \text{NHPI} + \text{Q=O} + {}^{\bullet}\text{OH} \qquad (34)$$

As no subsequent cage-reaction can produce alcohol (viz. reaction 13), NHPI addition also causes a reversed Q=O/CyOH ratio (see Fig. 6).

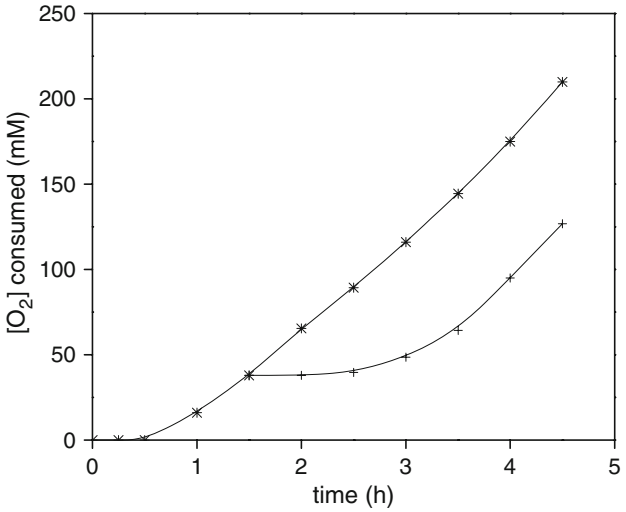

Fig. 5 Comparison of the 130 °C cyclohexane autoxidation activity of the immobilized NHPI catalyst (*, 0.1 mol%) and the activity of the supernatans, separated from the solid catalyst after 1.5 h (+) [47]

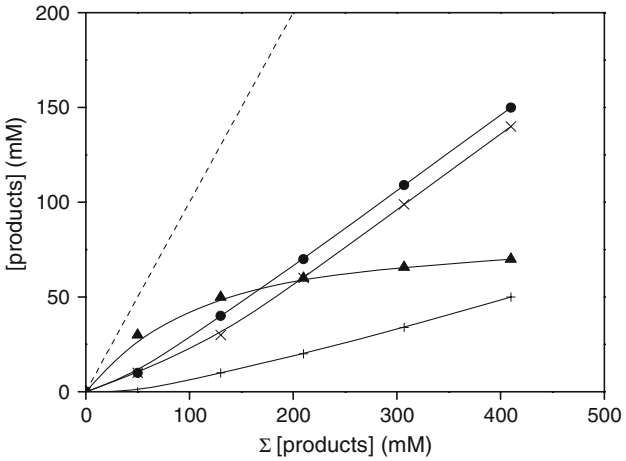

Fig. 6 Evolution of the cyclohexane autoxidation products at 130 °C in presence of 0.1 mol% immobilized NHPI as a function of the sum of products: CyOOH (▲), CyOH (×), Q=O (●), by-products (+) [47]. The dashed line represents the sum of products

Nevertheless, due to the nearly thermoneutral equilibrium (32) and the relatively high CyOOH concentrations, the PINO$^{\bullet}$/CyOO$^{\bullet}$ ratio is estimated to be only about 0.04, explaining why there is no stronger effect on the product distribution.

It has been observed that the homogeneous addition of cobalt or manganese salts has a synergetic effect on the oxidation rate [43]. This effect can be understood in the frame of the reaction mechanism above: Co or Mn salts decompose the hydroperoxide via a Haber–Weiss cycle (reactions 30 and 31), thereby not only enhancing the initiation but also causing a boost in the PINO$^{\bullet}$/ROO$^{\bullet}$ ratio. Indeed, shifting the equilibrium (32) towards the PINO$^{\bullet}$ radicals offers an opportunity to improve the performance

of the system both with respect to activity and selectivity. The possibility to combine the heterogeneous NHPI system with immobilized transition metal ions thus appears as an interesting route to design active and selective autoxidation catalysts in the future.

7 Conclusions

The hitherto accepted autoxidation mechanism showed a number of deficiencies. Foremost, the pathways assumed to lead to the major end products alcohol and ketone/aldehyde are much too slow to explain the observed high yields. Instead, the abstraction of the weakly bonded αH-atom from the primary hydroperoxide product appears to be a crucial reaction, directly yielding ketone/aldehyde. A subsequent cage-reaction between the nascent products of this hydroperoxide propagation produces alcohol. This step is rendered possible by the large amount of heat released in the previous abstraction step, causing the formation of a nano-sized hot-spot in the liquid phase. As a consequence, before the nascent products can diffuse away from each other, they can react together to produce alcohol. The efficiency of this cage-reaction also depends on the stability of the nascent products, as evaluated experimentally for several substrate types. In the case of cyclohexane autoxidation, this subsequent cage-reaction also produces cyclohexoxy radicals which are efficiently converted to ring-opened by-products. Transition metal ions such as Co(II) can efficiently take over the role of hydroperoxide destructor from the peroxyl radicals, thereby also acting as chain initiators. This however only causes a slight perturbation of the autoxidation chemistry—in contrast to the situation observed with chromium ions, which species appear to catalyze additional steps leading directly to (by-)products. Co-propagation of the radical chain by phthalimide-*N*-oxyl radicals, generated in situ from *N*-hydroxyphthalimide, cause a net destruction of hydroperoxide and an improved ketone to alcohol ratio as no subsequent cage-reaction can yield alcohol. A further exploration of the synergetic effects between both (heterogeneous) catalytic approaches should lead to more active and selective autoxidation catalysts.

Acknowledgments This work was performed in the frame of GOA, IDECAT, and CECAT projects, and the Belgian Program on Interuniversity Attraction Poles (IAP).

References

1. Sheldon RA, Kochi JK (1981) Metal-catalyzed oxidations of organic compounds. Academic Press, New York
2. Franz G, Sheldon RA (2000) Oxidation, in Ullmann's Encyclopedia of industrial chemistry. Wiley-VCH, Weinheim
3. Bhaduri S, Mukesh D (2000) Homogeneous catalysis, mechanisms and industrial applications. New York, Wiley
4. Tolman CA, Druliner JD, Nappa MJ, Herron N (1989) In: Hill CL (ed) Activation and functionalization of alkanes. Wiley, New York, p 303
5. Hermans I, Nguyen TL, Jacobs PA, Peeters J (2005) Chem Phys Chem 6:637
6. Hermans I, Jacobs PA, Peeters J (2006) J Mol Catal A: Chem 251:221
7. Hermans I, Jacobs PA, Peeters J (2006) Chem-Eur J 12:4229
8. Hermans I, Peeters J, Jacobs P (2007) J Org Chem 72:3057
9. Hermans I, Peeters J, Vereecken L, Jacobs P (2007) Chem Phys Chem 8:2678
10. Vereecken L, Nguyen TL, Hermans I, Peeters J (2004) Chem Phys Lett 393:432
11. Hermans I, Müller J-F, Nguyen TL, Jacobs PA, Peeters J (2005) J Phys Chem A 109:4303
12. Rowley DM, Lesclaux R, Lightfoot PD, Nozière B, Wallington TJ, Hurley MD (1992) J Phys Chem 96:4889
13. a) Druliner JD, Krusic PJ, Lehr GF, Tolman CA (1985) J Org Chem 50:5838; (b) Beckwith ALJ, Hay BP (1989) J Am Chem Soc 111:2674
14. Hermans I, Jacobs PA, Peeters J (2007) Chem-Eur J 13:754
15. Peeters J, Fantechi G, Vereecken L (2004) J Atmos Chem 48:59
16. Hermans I, Peeters J, Jacobs PA (2008) J Phys Chem A 112:1747
17. Buijs W, Raja R, Thomas JM, Wolters H (2003) Catal Lett 91:253
18. Vanoppen DL, De Vos DE, Genet MJ, Rouxhet PG, Jacobs PA (1995) Angew Chem Int Ed Engl 34:560
19. (a) Barrett PA, Sankar G, Carlow CRA, Thomas JM (1996) J Phys Chem 100:8977; (b) Maschmeyer T, Oldroyd RD, Sankar G, Thomas JM, Shannon IJ, Klepetko JA, Masters AF, Beattie JK, Catlow CRA (1997) Angew Chem Int Ed Engl 36:1642; (c) Sankar G, Raja R, Thomas JM (1998) Catal Lett 55:15
20. Sheldon RA, Wallau M, Arends IWCE, Schuchardt U (1998) Acc Chem Res 31:485
21. Breynaert E, Hermans I, Lambie B, Maes G, Peeters J, Maes A, Jacobs P (2006) Angew Chem Int Ed 45:7584
22. Hermans I, Breynaert E, Poelman H, De Gryse R, Liang D, Van Tendeloo G, Maes A, Peeters J, Jacobs P (2007) Phys Chem Chem Phys 9:5382
23. Ishii Y, Nakayama K, Takeno M, Sakaguchi S, Iwahama T, Nishiyama Y (1995) J Org Chem 60:3934
24. Iwahama T, Sakaguchi S, Nishiyama Y, Ishii Y (1995) Tetrahedron 36:6923
25. Ishii Y, Iwahama T, Sakaguchi S, Nakayama K, Nishiyama Y (1996) J Org Chem 61:4520
26. Ishii Y, Kato S, Iwahama T, Sakaguchi S (1996) Tetrahedron Lett 37:4993
27. Ishii Y (1997) J Mol Catal A: Chem 117:123
28. Yoshino Y, Hayashi Y, Iwahama T, Sakaguchi S, Ishii Y (1997) J Org Chem 62:6810
29. Kato S, Iwahama T, Sakaguchi S, Ishii Y (1998) J Org Chem 63:222
30. Iwahama T, Syojyo K, Sakaguchi S, Ishii Y (1998) Org Proc Res Dev 2:255
31. Sakaguchi S, Takase T, Iwahama T, Ishii Y (1998) Chem Comm 18:2037
32. Iwahama T, Sakaguchi S, Ishii Y (1998) Tetrahedron Lett 39:9059
33. Ishii Y, Sakaguchi S (1999) Catal Surv Jap 3:27
34. Iwahama T, Sakaguchi S, Ishii Y (2000) Chem Comm 7:613
35. Ishii Y (2006) Catal Today 117:105
36. Ishii Y, Sakaguchi S, Iwahama T (2001) Adv Synth Catal 343:393
37. Sheldon RA, Arends IWCE (2004) Adv Synth Catal 346:1051

38. Sheldon RA, Arends IWCE (2006) J Mol Catal A: Chem 251:200
39. Minisci F, Punta C, Recupero F, Fontana F (2002) G F Pedulli J Org Chem 67:2671
40. Amorati R, Lucarini M, Mugnaini V, Pedulli GF, Minisci F, Recupero F, Fontana F, Astolfi P, Greci L (2003) J Org Chem 68:1747
41. Minisci F, Recupero F, Pedulli GF, Lucarini M (2003) J Mol Catal A: Chem 204:63
42. Minisci F, Recupero F, Cecchetto A, Gambarotti C, Punta C, Faletti R, Paganelli R, Pedulli GF (2004) Eur J Org Chem 1:109
43. Recupero F, Punta C (2007) Chem Rev 107:3800
44. Hermans I, Vereecken L, Jacobs PA, Peeters J (2004) Chem Comm 9:1140
45. Hermans I, Jacobs P, Peeters J (2007) Phys Chem Chem Phys 9:686
46. Rajabi F, Clark JH, Karimi B, Macquarrie DJ (2005) Org Biomol Chem 3:725
47. Hermans I, Van Deun J, Houthoofd K, Peeters J, Jacobs PA (2007) J Catal 251:204